AIP | Journal of Renewable and Sustainable Energy

Energy, exergy, and cost analyses of a double-glazed solar air heater using phase change material

Mojtaba Edalatpour, Ali Kianifar, Kiumars Aryana, and G. N. Tiwari

Citation: Journal of Renewable and Sustainable Energy **8**, 015101 (2016); doi: 10.1063/1.4940433
View online: http://dx.doi.org/10.1063/1.4940433
View Table of Contents: http://scitation.aip.org/content/aip/journal/jrse/8/1?ver=pdfcov
Published by the AIP Publishing

JOURNAL OF RENEWABLE AND SUSTAINABLE ENERGY **8**, 015101 (2016)

Energy, exergy, and cost analyses of a double-glazed solar air heater using phase change material

Mojtaba Edalatpour,[1] Ali Kianifar,[1,a)] Kiumars Aryana,[1] and G. N. Tiwari[2]
[1]*Department of Mechanical Engineering, Ferdowsi University of Mashhad, Mashhad, Iran*
[2]*Center for Energy Studies, Indian Institute of Technology Delhi, Haus Khas, New Delhi 110016, India*

(Received 2 October 2015; accepted 8 January 2016; published online 22 January 2016)

In this paper, a double-glazed solar air heater (SAH) using paraffin wax as phase change material (PCM) was designed, fabricated, and tested under the climatic condition of Mashhad, Iran (latitude, 37° 28′ N and longitude, 57° 20′ E) during three typical days in the summer. The PCM stores solar radiation of the sun as latent and sensible heat during daytime and then restores such stored energy during the night. Exploitation of both first and second laws of Thermodynamics, the energy and exergy efficiencies of this system are assessed. According to the experiments undertaken, it is found that the daily energy efficiency of the system varies between 58.33% and 68.77%, whereas the daily exergy efficiency varies from 14.45% to 26.34%. Eventually, the economic analysis shows that the cost of 1 kg of heated air utilizing double-glazed SAH would be 0.0036$. © *2016 AIP Publishing LLC*. [http://dx.doi.org/10.1063/1.4940433]

I. INTRODUCTION

Population growth precipitates the countries into consuming more energy to provide the essential preliminary demands of their people such as water, food, and so on. Unfortunately, the vast majority of industries situated in these populated countries heavily depend on the fossil fuels. The detrimental consequences of fossil fuels consumptions are not hidden from views these days. They are implicated in earth's temperature increment, causing incurable diseases, vegetation and animal extinction, and so on.[1] Therefore, to address such insurmountable problems that threat our environment, some measurements should be taken. One of the fruitful steps that are being augmented is to exploit renewable energy. Renewable energy is called to the source of energies that can be replenished by nature, namely, solar, the wind, tides, and so on, that are inexhaustible.

Solar energy is classified as one sort of the renewable energy sources that are abundant, free, and clean. The amount of radiation that our earth receives from the sun is estimated to be 174 000 TW that is 40 000 times larger than our needs.[2] Hence, taking into account of using solar radiation as a reliable source to produce energy for domestic and industrial purposes is not out of reach. One of the applications that can be used for domestic intentions by the solar radiation is solar air heater (SAH). The SAHs can be used in various conditions, namely, drying, ventilation, hot water supply, and so on.[3]

Solar air heaters fall into different categories. For instance, one of the common classifications of the SAH is exploitation of solar air heater with and without phase change material (PCM).[4] PCM is a unit in the apparatus located within the system that stores solar radiation from the sun during daytime by melting to liquid phase. Depending on PCM specific applications, a number of substances can be employed as the ingredient for the PCM such as paraffin wax, capsule (AC27), silver, and so on.[5]

[a)]Authors to whom correspondence should be addressed. Electronic addresses: a-kiani@um.ac.ir and gntiwari@ces.iitd.ernet.in

Vijaya Venkata Raman *et al.*[6] reviewed 12 different solar air heaters that were fabricated and used for drying various products, namely, onions, fruits, and so on. Their review revealed that exploitation of solar air heaters is appropriate for drying purposes. Also, the quality of products dried by those solar air heaters is higher in comparison with that of dried by fossil fuels facilities.

Kumar *et al.*[7] reviewed heat transfer and friction characteristics of a multiplicity of artificially roughened solar air heaters. They expressed different ways that could be used to improve heat transfer and as a result performance enhancement of these solar systems.

Tyagi *et al.*[8] compared energy and exergy efficiencies of three different solar air heater collector arrangements with and without thermal energy storage materials, using first and the second laws of Thermodynamics. Their results showed that utilization of thermal energy storage materials such as paraffin wax and hytherm oil can soar both energy and exergy efficiencies of their systems simultaneously. Additionally, they mentioned that these efficiencies are slightly higher for the system used paraffin wax, compared to the one that exploited hytherm oil.

Singh *et al.*[9] conducted a research to illuminate the exergy efficiency of a solar air heater that had discrete V-down rib roughness on its absorber plate. They perceived that not only did their system performed better from energy and exergy points of view, but also it is extremely appropriate to be used for the condition that Reynolds number is lower than 18 000. However, using their system for higher Reynolds numbers will lead to more pump power consumption that is unfavorable.

Bouadila *et al.*[10] manufactured a novel solar air heater with packed-bed latent storage energy to evaluate the nocturnal performance of their apparatus. They reported that the daily energy efficiency varied between 32% and 45%, while the daily exergy efficiency ranged from 13% to 25%.

Sabzpooshani *et al.*[11] investigated the exergetic performance of a single pass baffled solar air heater. They realized that exergy efficiency was the superior criterion for performance evaluation. Yet another, the more intense the solar radiation is, the higher exergy efficiency will be.

Bayrek *et al.*[12] fabricated five different solar air heaters with and without porous baffles to assess the energy and exergy efficiencies. Their experiments anticipated that using a solar air heater with a thickness of 6 mm and an air mass flow rate of 0.025 kg/s had the maximum efficiencies, while the one that no baffles were inserted in had the lowest efficiencies. Furthermore, the energy and exergy efficiencies for their five various solar systems varied between 39.35%–77.57% and 21.55%–54.54%.

Bahrehmand and Ameri[13] mathematically studied the energy and exergy efficiencies of two different solar air heaters. They deduced that collector that triangular fins were inserted in was more efficacious than that of rectangular fins from energy and exergy perspectives.

Yadav *et al.*[14] analytically appraised the exergetic performance of a solar air heater provided with protrusions arranged in arc fashion on its absorber plate. They figured out that using such solar facility is appropriate for Reynolds number less than 20 000, while for Reynolds number greater than 20 000, the exergetic efficiency will decline due to considerable increase in pumping power required by fan.

Bahrehmand *et al.*[15] mathematically conducted an investigation to study various solar air heaters utilized under force convection condition from energy and exergy standpoints. They reported that the system made of the thin metal sheet is preferable, at high Reynolds number ($\mathrm{Re} > 22\,000$).

Aloyem Kaze and Tchinda[16] investigated the energetic and exergetic performance of a downward flat plate collector, an unglazed absorber collector and an artificial rough surface collector developing mass, energy, and exergy balance equations. They mentioned that the daily exergy output rate varies conversely with the mass flow rate per unit area. What is more, they reported that their artificially rough surface collector had fourfold higher exergy efficiency, in contrast to that of conventional solar air heater at Reynolds number around ($\mathrm{Re} = 4000$).

In this research paper, a double-glazed SAH equipped with phase change material (paraffin wax) constructed and tested for the first time under the meteorological condition of Mashhad,

Iran. The objective of the current study is to present an efficient SAH device, which is capable of operating for nocturnal use. Taking advantage of latent heat of paraffin wax with a special configuration beneath the absorber plate enables us to store heat during the day light and release the accumulated heat to the flowing air in the night. To trap more heat and minimize the heat loss, a double-glazed SAH is employed in this study and from the economic prospect, a thorough cost analysis is presented for the given SAH. Hence, to evaluate such solar air heater functioning during daytime and night, the energy and exergy analyses (1st and 2nd law of Thermodynamics) are applied, as well as cost analysis, to satisfy the aim of this study. Also, review of the literature shows that no similar endeavor has been done on this type of solar air heater using paraffin wax as a thermal storage unit with a double-glazed cover. Furthermore, no cost analysis has ever been accomplished on this type of solar air heater.

II. EXPERIMENTAL SET-UP

A double-glazed solar air heater, depicted in Fig. 1, was designed and constructed to investigate the charging and discharging processes. The tests were carried out under the meteorological condition of Mashhad, Iran (latitude, 37° 28′ N and longitude, 57° 20′ E) that has a semi-arid climatic condition. Different parameters, namely, mass flow rate, ambient, and operating temperatures, were measured to evaluate the energy and exergy efficiencies of the system.

The experimental apparatus represents a packed-bed of solid paraffin wax as PCM enclosed in rectangular solid shape which adhered firmly underneath of the dull black absorber plate and fixed with galvanize matrix. The solid paraffin wax confined in collector box which covers all the bottom space of absorber plate and weigh around 15 kg. It is proved that the air gap between PCM and the absorber plate would decrease the heat transfer rate to PCM. Rectangular solid shape paraffin wax has an average thickness of 2.5 cm, 110 cm, and 60 cm length and width, respectively. The PCM is the prominent component of the solar air heater collector since it absorbs solar radiation during days and stores them as sensible and latent heat. Therefore, the system can be exploited for nocturnal purposes and the conditions which no sufficient solar radiation exist, as well. The length, width and the total volume of the collector are 1.1 m, 0.6 m, and 0.112 m^3, respectively. Two 4 mm transparent glass covers were placed 0.05 m and 0.1 m apart from the absorber plate that was built of 0.0125 m galvanized sheet. A 0.05 m thick glass wool insulation, with thermal conductivity 0.04 W $(m\ K)^{-1}$, was made to cover the lateral and bottom walls of the collector to diminish heat loss. This heat loss may occur during tests from walls and could lead to energy and exergy efficiencies reduction. Additionally, to eliminate any feasible air leakages from the SAH to the surrounding, gaps that permit the inlet air flow to escape were sealed by aquarium adhesive. To enhance the convective heat transfer within the system, crushed coal was sprinkled on the absorber plate. Moreover, the absorber plate was painted in black and

FIG. 1. Schematic view of the double-glazed solar air heater (SAH) under operation.

inclined at an inclination of about 37° to the horizontal surface to absorb the maximum available solar radiation.

A. Measurement procedures

The charging process commences when the absorber plate receives solar radiation at 6:00 a.m. to 5:00 p.m. During this period, the inlet and outlet were kept closed. The amount of solar radiation and wind speed were obtained from a local meteorological station in Mashhad, Iran (see Figs. 2 and 3). On the other hand, the discharging process starts at 5:00 p.m. to 6:00 a.m. (the next day), and during this time span, the inlet and outlet were opened. To establish air flow, a low-power fan (VMA-10S2S) exploited to blow the air.

The inlet mass flow rate of air was measured using a Pitot Tube Anemometer (EXTECH, HD350). The inlet and outlet air temperatures of the solar air heater and the PCM temperature were assessed with the assistance of K-type thermocouples (Thermometer, ST-612). The experimental values were recorded every 30 min. The thermophysical properties of the air at 300 K and PCM (Paraffin wax) in both liquid and solid phases are tabulated in Table I.

III. THEORETICAL BACKGROUND

A. Energy analysis of the SAH

According to the first law of thermodynamics, the energy analysis of the solar air heater is defined as[18]

$$Q_A = Q_u + Q_{st} + Q_{los}, \tag{1}$$

where Q_A, Q_u, Q_{st}, and eventually Q_{los} are the absorbed, useful, stored, and lost energies, respectively.

To calculate the useful heat gain, Duffie and Beckman[19] propounded an equation

$$Q_u = \dot{m}C_p(T_{out} - T_{in}), \tag{2}$$

where

$$\dot{m} = \rho V_{av} S. \tag{3}$$

V_{av} and S are mean air velocity and cross sectional area of the duct at the inlet of the solar air heater, respectively.

The radiation absorbed flux of the PCM is

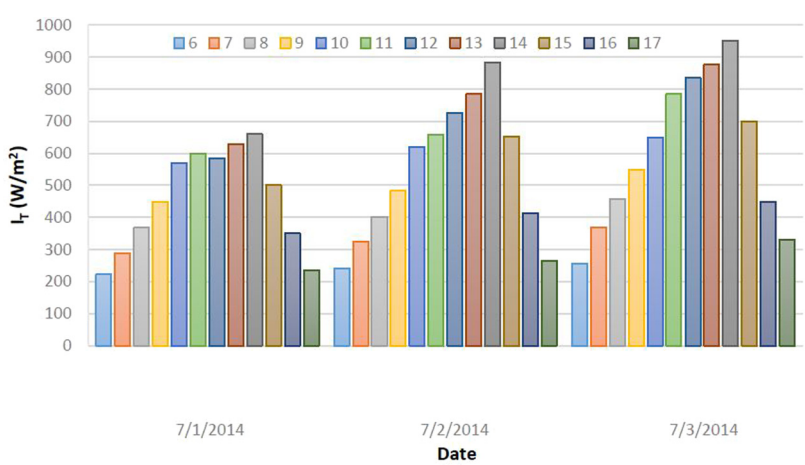

FIG. 2. Hourly variations of the local solar radiation from the 1st to 3rd of July 2014.

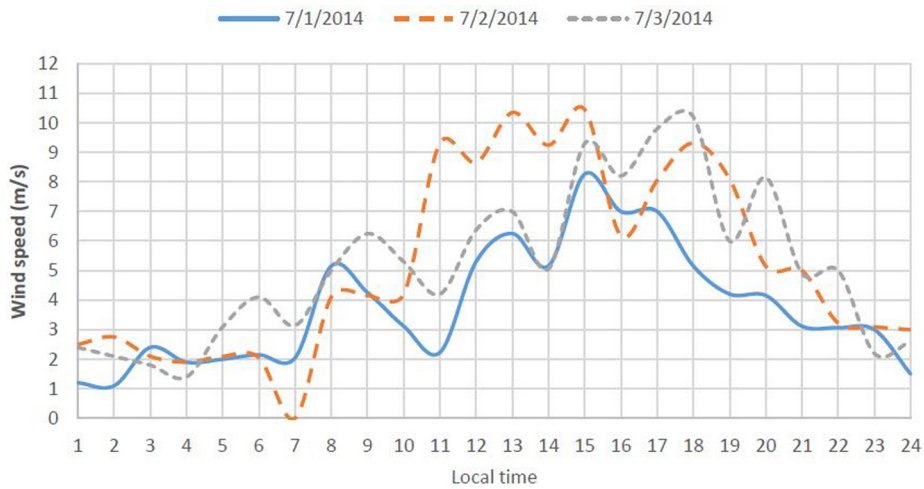

FIG. 3. Hourly variations of local wind speed from the 1st to 3rd of July 2014.

$$Q_A = A_p(\alpha\tau)I_T, \tag{4}$$

where $(\alpha\tau)$ is the optical efficiency (η_o).[19]

The stored heat flux for charging and discharging phases is determined by

$$Q_{ch} = [m_{PCM}C_{p,s}(T_m - \bar{T}_{ini\_ch,PCM}) + m_{PCM}L + m_{PCM}C_{p,l}(\bar{T}_{fin\_ch,PCM} - T_m)]/\Delta t_{ch}, \tag{5}$$

$$Q_{dis} = [m_{PCM}C_{p,l}(T_m - \bar{T}_{fin\_dis,PCM}) + m_{PCM}L + m_{PCM}C_{p,s}(\bar{T}_{ini\_dis,PCM} - T_m)]/\Delta t_{dis}. \tag{6}$$

The heat flux lost from the collector to the ambient by conduction, convection, and infrared radiation can be given by[10]

$$Q_{los} = U_{los}A_c(\bar{T}_p - T_a), \tag{7}$$

where U_{los} is the collector overall heat loss coefficient and defined as below

$$U_{los} = U_t + U_b + U_e, \tag{8}$$

$$U_t = (1/(h_{c,P-g} + h_{r,P-g}) + 1/(h_w + h_{r,g-a}))^{-1}. \tag{9}$$

The flow is laminar during the charging phase. Hence, the suitable correlation for estimation of the Nusselt number is presented as[20]

$$Nu_{ch} = 0.68 + \frac{(0.67 \times Ra^{1/4})}{\left(1 + (0.492/Pr)^{9/16}\right)^{4/9}} \quad [Ra \leq 10^{+9}]. \tag{10}$$

TABLE I. Thermal properties of air and PCM.[17]

Material	Melting point (K)	Heat of fusion (kJ/kg)	Specific heat (kJ/kg K) Liquid/Gas	Specific heat (kJ/kg K) Solid	Density (kg/m^3) Liquid/Gas	Density (kg/m^3) Solid	Thermal conductivity (W/m K) Liquid/Gas	Thermal conductivity (W/m K) Solid
Air (at 298.15 K)	…	…	1.0048	…	1.137	…	0.0249	…
Paraffin wax	326	184.5	2.89	2.384	775	900	0.25	0.15

The flow is turbulent during discharging phase. Hence, the appropriate correlation for estimation the Nusselt number is posed as[20]

$$Nu_{ch} = 0.68 + \frac{(0.67 \times Ra^{1/4})}{\left(1 + (0.492/Pr)^{9/16}\right)^{4/9}} \quad \left[Ra \leq 10^{+9}\right], \tag{11}$$

$$h_{c,P-g} = Nu(\lambda/t), \tag{12}$$

$$h_{r,P-g} = \left(\frac{\sigma(T_p + T_g)\left(T_p^2 + T_g^2\right)}{\left(\frac{1}{\varepsilon_p} + \frac{1}{\varepsilon_g} - 1\right)}\right). \tag{13}$$

The external convective and radiative heat transfer due to the wind velocity is proposed by Hottel and Woertz[10]

$$h_w = 5.67 + 3.86V_\infty, \tag{14}$$

$$h_{r,g-a} = \varepsilon_g \sigma(T_g + T_{sky})(T_g^2 + T_{sky}^2), \tag{15}$$

where T_{sky} can be calculated by the following equation:[21]

$$T_{sky} = 0.0552\, T_a^{1.5}. \tag{16}$$

Heat loss coefficient for bottom and the lateral walls of the solar air heater are

$$U_b = \lambda_i/\delta_b, \tag{17}$$

$$U_e = ((L_1 + L_2)L_3\lambda_i)/(L_1L_2\delta_e), \tag{18}$$

where L_1, L_2, and L_3 are length, width, and height of the SAH, respectively.

The thermal efficiencies of the solar air heater according to the first law of thermodynamics can be defined as the ratio between the useful energy (Q_u) and the solar radiation incident on the collector

$$\eta_{daily} = \left(\int_{dis} Q_{dis}\right) \Big/ \left(\int_{ch} A_c I_T\right). \tag{19}$$

The dimensionless parameters mentioned above are defined as[22]

$$\begin{aligned} Ra &= \frac{g\beta\Delta TL^3}{\alpha v}, \\ Pr &= \frac{\nu}{\alpha}, \\ Re &= \frac{VD_h}{v}. \end{aligned} \tag{20}$$

B. Exergy analysis of the SAH

To develop the exergy analysis based on the second law of thermodynamics for the discussed problem, multiplicity of assumptions are needed to consider:

1. Steady-state, steady flow operation.
2. The fluid, air, is an ideal gas with constant physical properties.

3. The humidity of the air is negligible.
4. No chemical and nuclear reactions happen.
5. Although the system installed with an inclination angle about 36°, potential and kinetic energy differences are negligible.

The general form of the second law of thermodynamics, exergy balance equation, is[23]

$$Ex_{in} = Ex_{out} + Ex_{los} + Ex_d + Ex_{st}, \tag{21}$$

where Ex_{in}, Ex_{out}, Ex_{los}, Ex_d, and eventually Ex_{st} are the inlet, outlet, leakage, destroyed, and stored exergy, respectively.

The inlet exergy with flowing air flow is given by

$$Ex_{in}(air\,flow) = \dot{m}C_p\left(T_{in} - T_a\left(1 + \ln\left(\frac{T_{in}}{T_a}\right)\right)\right) + \dot{m}RT_a\ln\left(\frac{P_{in}}{P_a}\right). \tag{22}$$

The outlet exergy is given by

$$Ex_{out}(air\,flow) = \dot{m}C_p\left(T_{out} - T_a\left(1 + \ln\left(\frac{T_{out}}{T_a}\right)\right)\right) + \dot{m}RT_a\ln\left(\frac{P_{out}}{P_a}\right). \tag{23}$$

The absorbed solar radiation exergy can be obtained as

$$Ex_{in}(solar\,radiation) = I_T\left[1 - \frac{4}{3}\left(\frac{T_a}{T_s}\right) + \left(\frac{T_a}{T_s}\right)^4\right], \tag{24}$$

where $T_s = 6000\,K$. To evaluate the total inlet exergy, both Equations (21) and (22) must be summed.[10,12]

The leakage exergy, Ex_{los}, is taken place, as a result of heat leakage from the absorber to the surroundings and can be expressed as[23]

$$Ex_{los} = -U_{los}A_c\left[(T_p - T_a) - (T_a + 273)\ln\frac{(T_p + 273)}{(T_a + 273)}\right]. \tag{25}$$

The destroyed exergy, Ex_d, is comprised of three different terms[24,25]

1. the absorber plate surface and sun temperature difference
2. the duct pressure drop
3. the heat transfer from absorber plate surface to the fluid.

$$Ex_d(p - s) = -\eta_o I_T A_c T_a\left(\left(\frac{1}{T_p}\right) - \left(\frac{1}{T_s}\right)\right), \tag{26}$$

$$Ex_d(\Delta P) = -(\Delta P T_a/\rho)\left(T_a\ln\left(\frac{T_{out}}{T_a}\right)\right)\Big/(T_{out} - T_{in}), \tag{27}$$

$$Ex_d(p - f) = -\dot{m}C_pT_a\left(\ln\left(\frac{T_{out}}{T_{in}}\right) - \left(\frac{T_{out} - T_{in}}{T_p}\right)\right). \tag{28}$$

The stored exergy is composed of discharging process for the charging and discharging state and can be conveyed as[26]

$$Ex_{dis} = \left[\begin{array}{c} m_{PCM}C_{p,l}\left(T_m - \bar{T}_{fin_{dis},PCM} - T_a \ln\left(\frac{T_m}{\bar{T}_{fin_{dis},PCM}}\right)\right) + m_{PCM}L\left(1 - \left(\frac{T_a}{T_m}\right)\right) \\ + \\ m_{PCM}C_{p,s}\left(\bar{T}_{ini_{dis},PCM} - T_m - T_a \ln\left(\frac{\bar{T}_{ini_{dis},PCM}}{T_m}\right)\right) \end{array} \right] \Big/ \Delta t_{dis}. \tag{29}$$

Eventually, the daily exergy efficiency of the SAH can be calculated by the following equation:[12]

$$\psi_{daily} = \left(\int_{dis} Ex_{dis}\right) \Big/ \left(\int_{ch} Ex_{in}(absorbed)\right). \tag{30}$$

C. Uncertainty analysis

To prove the accuracy of the experiments performed on the double-glazed SAH, uncertainty analysis is obligatory from the technical perspective. The errors occurred during tests could be consisted of both sensitivity of the equipment and measurement uncertainties.[27,28]

The uncertainty of the measurement equipment is as follows:

- Sensitiveness of the thermocouples is $\pm$ 0.01 °C.
- Sensitiveness of the Pitot Tube Anemometer is $\pm$ 1 Pa.

The values of uncertainty for the mass flow rate, the heat rate, and the energy efficiency can be calculated exploiting following equations:[29,30]

$$\frac{w_{\dot{m}}}{\dot{m}} = \sqrt{\left[\left(\frac{w_{\dot{m}}}{V_m}\right)^2 + \left(\frac{w_{T_a}}{T_a}\right)^2 + \left(\frac{w_{P_a}}{P_a}\right)^2\right]}, \tag{31}$$

$$\frac{w_Q}{Q} = \sqrt{\left[\left(\frac{w_{\dot{m}}}{\dot{m}}\right)^2 + \left(\frac{w_{(T_{out}-T_{in})}}{T_{out}-T_{in}}\right)^2\right]}, \tag{32}$$

$$\frac{w_{\dot{m}}}{\eta} = \sqrt{\left[(w_{\dot{m}} \times \dot{m})^2 + \left(\frac{w_{(T_{out}-T_{in})}}{(T_{out}-T_{in})}\right)^2 + \frac{w_{I_T}}{I_T}\right]}. \tag{33}$$

Using the above-mentioned equations, the total uncertainty values of the SAH are 0.0035, 0.031, and 0.031 for mass flow rate, the heat rate, and the energy efficiency, respectively.

D. Economic analysis

Exploitation of economic analysis would enable us to have a deep understanding of 1 kg hot air production cost using SAH. To develop an acceptable cost prediction, several consequential parameters, namely, sinking fund factor (SFF), annual salvage value (ASV), annual maintenance cost, and interest rate per year, should be deemed as well as the capital cost of the SAH.

The capital recovery factor (CRF) is defined in terms of the interest per year, i, and also the number of life years of the system, n (Ref. 31)

$$CRF = \frac{i(1+i)^n}{(1+i)^n - 1}. \tag{34}$$

The interest per year i and the number of life years of the SAH n are taken 12% and 10, respectively.

Fixed annual cost (FAC) becomes

$$FAC = P(CRF), \tag{35}$$

where P is the capital cost of SAH. The capital cost represents the cost of structure made of galvanized sheet as well as the cost of PCM, glass cover, insulation, labor, paint, providing crushed coal and a DC fan. In this investigation, the capital cost P becomes around 113$.

By considering the salvage value of system S equal to 20% of the capital cost

$$S = 0.2 \times P. \tag{36}$$

SFF and ASV can be given, respectively, as below[32]

$$SFF = \frac{i}{(1+i)^n - 1}, \tag{37}$$

$$ASV = (SFF) \times S. \tag{38}$$

Annual maintenance operational cost (AMC) of the system, AMC, comprised of cleaning the glass cover from dust, maintenance of DC fan, and the cost of electricity (CE). Thus, 15% of fixed annual cost (AC) is taken as maintenance cost

$$AMC = 0.15(FAC) + CE(CRF). \tag{39}$$

Therefore, the AC is determined[30]

$$AC = FAC + AMC - ASV. \tag{40}$$

Eventually, the cost of 1 kg hot supply air can be calculated as

$$CPL = \frac{AC}{M}. \tag{41}$$

where M is the average annual hot air supplied by the SAH. In this study, the amount of M is evaluated with respect to the characteristics of the fan employed.

IV. RESULTS AND DISCUSSION

In this paper, experiments were carried out to evaluate the energy and exergy performances of a double-glazed solar air heater for three clear sky days during a period in July 2014. Experiments were conducted under the climatic condition of Mashhad, Iran. As shown above, the local solar radiation and wind velocity fluctuate approximately between 250–950 W/m^2 and 1–11 m/s, respectively. For triple test days, the maximum solar radiations were recorded at around 2 p.m. while the maximum wind velocities blew during 11 a.m. to 6 p.m.

Fig. 4 depicts the variation of the ambient, outlet flow and PCM temperatures for three different test days from 1st to 3rd of July 2014 for both charging and discharging processes. As is obvious, ambient temperatures of these triple days have the minimum values while the values of the PCM temperatures are the maximum. During charging process, air enters the double-glazed solar air heater with ambient temperature. The temperature of the absorber plate that receives the solar radiation of the sun increases and leads into rising in both inlet flow and PCM temperatures. On the other hand, during the discharging process, the inlet air that has the ambient temperature gets heated by the energy absorbed during charging process within the PCM. However, the temperature of the PCM shown in Fig. 4 is relatively higher compared to that of the outlet flow since the PCM that is fixed under the absorber plate has higher specific heat capacity (C_p), and has longer time for heat transfer, as well.

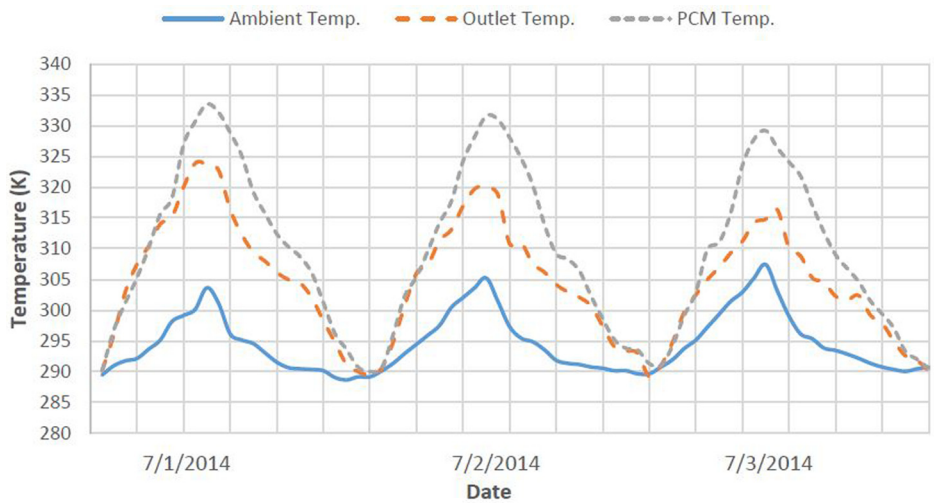

FIG. 4. Comparison of the ambient, outlet, and PCM temperatures of the double-glazed SAH from 1st to 3rd of July 2014.

Fig. 5 denotes the amount of absorbed, stored, useful, and loss heat rates for 1st to 3rd of July 2014. The amount of heat absorbed and lost (released) are shown by positive and negative signs on Y-axis. As can be seen, the amounts of useful heat rate are larger in comparison with the heat stored in the PCM for all of the test days whereas the rates of heat loss are the lowest. To put it differently, a part of absorbed heat received from the sun (during charging process) transfers to the air in the SAH's conduit and a great deal of the heat stores in the PCM. Also, it is obvious that during nights (discharging process), heat that were stored in the PCM release and lead to increment of the inlet air flow temperature and simultaneously plummeting the PCM temperature. Yet another, the amount of heat lost from the system is approximately negligible for all three test days. Therefore, it can be concluded that the amount of insolation employed for the double-glazed SAH is adequate.

Fig. 6 shows the values of daily energy and exergy efficiencies of the double-glazed SAH for three different test days. Based on the experimental data recorded, the maximum daily energy and exergy values are attained for 2nd of July. The daily energy and exergy efficiencies values for 2nd of July are 68.77% and 26.34%, respectively. While the minimum values for both energy and exergy efficiencies are acquired for 1st of July. The daily energy and exergy

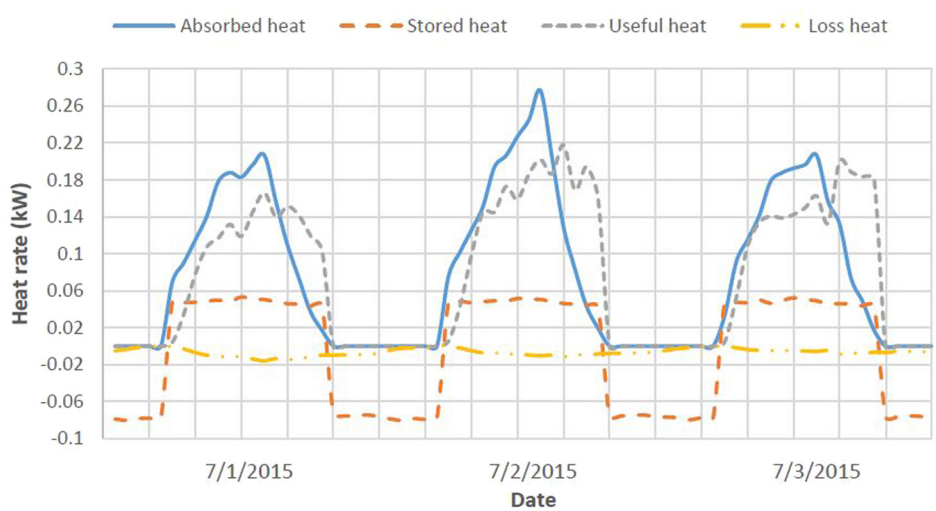

FIG. 5. Fluctuations of the absorbed, stored, useful, and loss heat rates of the SAH from 1st to 3rd of July 2014.

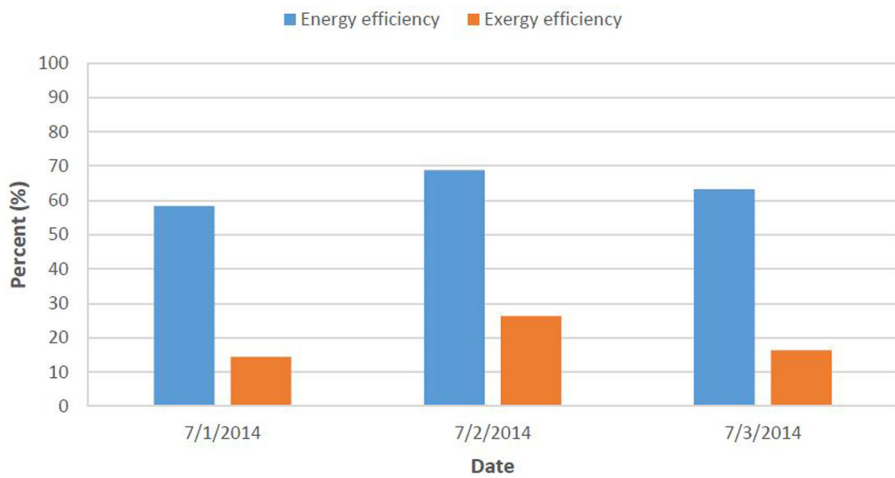

FIG. 6. Daily energy and exergy efficiency values of the SAH between 1st and 3rd of July 2014.

efficiencies for 1st of July are 58.33% and 14.45%, respectively. The reason for which such variation in energy and exergy values happened from 1st to 3rd of July can be associated with different solar radiation intensity values and reduction in absorbed energy that lead to declining in both energy and exergy efficiencies. It appears that the exploitation of a double-glazed top along with perfectly insulation of sides of the apparatus resulted in a higher efficiency compared to other studies. It should be noted that the configuration of PCM blocks which were completely connected beneath the absorber plate, has also contributed a significant part to the reduction of lost heat and therefore ameliorated the efficiency.

The total cost of construction of the double-glazed SAH in US$ is estimated and tabulated in Table II. Moreover, different components purchased for fabrication of the double-glazed SAH can be seen in Table II in detail.

The results of cost analysis for the present double-glazed SAH are provided in Table III. Considering different parameters, namely, CRF, FAC, SFF, ASV, and AMC, it is found that heating 1 kg of air using double-glazed SAH would be predicted approximately 0.0036$.

However, it should be noted that the interest per year i, number of life years of the double-glazed SAH n, and the cost of electricity per 1 kWh are deemed 12%, 10, and 0.0125 US $ for calculations that have been mentioned in Table III, respectively.

TABLE II. Cost of components used for the SAH.

Materials	Number/amount	Estimated cost ($)
Glass	2	5.7
Absorber plate	1	6.5
Paraffin wax (PCM)	15 kg	32.5
Insolation	1.3 m	5.1
Fan	1	9.60
Galvanized sheet	2 m^2	13
Crushed coal	0.02 kg	0.03
Black-paint spray	1	1
Aquarium adhesive	1	1.33
Welding, riveting, screwing, and drilling	…	35
Electrical devices	…	3.5
Total cost of construction (P)		113.3

TABLE III. The results of the cost analysis of the SAH.

Interest rate (%)	Mass flow rate (kg)	CRF	FAC	SFF	ASV	AMC	AC	CPL ($/kg)
12	7905	0.177	20.05	0.057	1.29	9.725	25.65	0.0036

V. CONCLUSIONS

In this paper, a double-glazed SAH designed, constructed, and experimentally tested under the meteorological climate of Mashhad, Iran (latitude, 37° 28′ N and longitude, 57° 20′ E). The 1st and 2nd laws of Thermodynamics are applied to assess the energy and exergy efficiencies of the system. The principal conclusions of this experimental study can be drawn as below:

1. The daily energy efficiency of the double-glazed SAH varies between 58.33% and 68.77%.
2. The daily exergy efficiency of the double-glazed SAH varies between 14.45% and 26.34%.
3. The cost of heating would be 0.0036$ for producing 1 kg hot air.
4. Paraffin wax is a suitable substance to be utilized as a PCM for the solar air heaters due to:
   - Its potential to store the energy of the sun during daytime successfully.
   - Its capacity to release the energy absorbed during night to warm up the air enters the double-glazed SAH appropriately.

ACKNOWLEDGMENTS

The fourth author, Professor Dr. G. N. Tiwari, would like to express his appreciation of the Department of Science and Technology, Government of India, India for their partial financial support of this work.

NOMENCLATURE

A_C	surface area of the collector, m^2
A_p	surface area of the absorber plate, m^2
C_p	specific heat of air, J/kg K
D_h	hydraulic diameter, m
Ex_d	destroyed exergy, W
Ex_{in}	inlet exergy, W
Ex_{los}	loss exergy, W
Ex_{out}	outlet exergy, W
Ex_{st}	stored exergy, W
h	heat transfer coefficient, W/m^2 K
h_c	convection eat transfer coefficient, W/m^2 K
h_r	radiation heat transfer coefficient, W/m^2 K
h_w	wind convection coefficient, W/m^2 K
i	interest per year
I_T	solar radiation, W/m^2
L	Latent heat, J/kg
L_1	collector length, m
L_2	collector width, m
L_3	collector depth, m
$\dot{m}$	mass flow rate, kg/s
n	number of life years
Nu	Nusselt number
P	fluid pressure, Pa
Pr	Prandtl number
Q	heat, W

R	universal gas constant, J/kg K
Ra	Rayleigh number
Re	Reynolds number
S	section area of the solar air heater, m^2
t	time, s
T	temperature, K
T_m	melting temperature, K
U	heat loss coefficient, W/m^2 K
V	velocity, m/s

GREEK SYMBOLS

α	absorptance
δ_b	bottom insulation thickness, m
δ_e	edge insulation thickness, m
Δ	difference in time
ε	emissivity
η	energy efficiency (%)
η_o	optical yield
λ	thermal conductivity, W/m K
λ_i	Insulation thermal conductivity, W/m K
μ	PCM dynamic viscosity, N s/m^2
μ_s	PCM dynamic viscosity at T_{pcm}, N s/m^2
ρ	density, kg/m^3
σ	Stefan-Boltzmann constant, W/m^2 K^4
τ	transmittance
ψ	exergy efficiency (%)

SUBSCRIPTS

a	ambient
A	absorbed
av	Mean
b	bottom
c	cold
ch	charging
dis	discharging
e	edge
fin	final
g	glasses
H	hot
in	inlet
ini	initial
l	liquid phase
los	leakage
out	outlet
p	absorber plate
PCM	phase change material
s	solid phase
st	storage
u	useful

[1]A. S. Yadav and J. L. Bhagoria, "Heat transfer and fluid flow analysis of solar air heater: A review of CFD approach," Renewable Sustainable Energy Rev. **23**, 60–79 (2013).

[2]S. Kooli, S. Bouadila, M. Lazaar, and A. Farhat, "The effect of nocturnal shutter on insulated greenhouse using a solar air heater with latent storage energy," Sol. Energy **115**, 217–228 (2015).
[3]A. S. Yadav and J. L. Bhagoria, "A CFD based thermos-hydraulic performance analysis of an artificially roughened solar air heater having equilateral triangular sectioned rib roughness on the absorber plate," Int. J. Heat Mass Transfer **70**, 1016–1039 (2014).
[4]A. Saxena, Varun, and A. A. El-Sebaii, "A thermodynamic review of solar air heaters," Renewable Sustainable Energy Rev. **43**, 863–890 (2015).
[5]A. S. Yadav and M. K. Thapak, "Artificially roughened solar air heater: Experimental investigations," Renewable Sustainable Energy Rev. **36**, 370–411 (2014).
[6]S. VijayaVenkataRaman, S. Iniyan, and R. Goic, "A review of solar drying technologies," Renewable Sustainable Energy Rev. **16**, 2652–2670 (2012).
[7]A. Kumar, R. P. Saini, and J. S. Saini, "Heat and fluid flow characteristics of roughened solar air heater ducts—A review," Renewable Energy **47**, 77–94 (2012).
[8]V. V. Tyagi, A. K. Pandey, G. Giridhar, B. Bandyopadhyay, S. R. Park, and S. K. Tyagi, "Comparative study based on exergy analysis of solar air heater collector using thermal energy storage," Int. J. Energy Res. **36**, 724–736 (2012).
[9]S. Singh, S. Chander, and J. S. Saini, "Exergy based analysis of solar air heater having discrete V-down rib roughness on absorber plate," Energy **37**, 749–758 (2013).
[10]S. Bouadila, S. Kooli, M. Lazaar, S. Skouri, and A. Farhat, "Performance of a new solar air heater with packed-bed latent storage energy for nocturnal use," Appl. Energy **110**, 267–275 (2013).
[11]M. Sabzpooshani, K. Mohammadi, and H. Khorasanizadeh, "Exergetic performance evaluation of a single pass baffled solar air heater," Energy **64**, 697–706 (2014).
[12]F. Bayrek, H. F. Oztop, and A. Hepbasli, "Energy and exergy analyses of porous baffles inserted solar air heater for building applications," Energy Build. **57**, 338–345 (2013).
[13]D. Bahrehmand and M. Ameri, "Energy and exergy analysis of different solar air collector system with natural convection," Renewable Energy **74**, 357–368 (2015).
[14]S. Yadav, M. Kaushal, and S. Varun, "Exergetic performance evaluation of solar air heater having arc shape oriented protrusions as roughness element," Sol. Energy **105**, 181–189 (2014).
[15]D. Bahrehmand, M. Ameri, and M. Gholampour, "Energy and exergy analysis of different solar air collector systems with forced convection," Renewable Energy **83**, 1119–1130 (2015).
[16]C. V. Aloyem Kaze and R. Tchinda, "Exergy analysis of an air solar heater," Int. J. Exergy **11**(1), 19–34 (2012).
[17]S. Himran, A. Suwono, and G. A. Mansoori, "Characterization of Alkanes and Paraffin waxes for application as phase change energy storage medium," Energy Sources **16**, 117–128 (1994).
[18]D. Atheaya, A. Tiwari, G. N. Tiwari, and I. M. Al-Helal, "Analytical characteristic equation for partially covered photovoltaic thermal (PVT) compound parabolic concentrator (CPC)," Sol. Energy **111**, 176–185 (2015).
[19]J. A. Duffie and W. A. Beckman, *Solar Engineering of Thermal Processes*, 2nd ed. (John Wiley and Sons, New York, USA, 1991).
[20]F. P. Incropera, D. P. DeWitt, T. L. Bergman, and A. S. Lavine, *Fundamentals of Heat and Mass Transfer*, 6th ed. (John Wiley and Sons, New York, USA, 2007).
[21]M. Al-Nimr and M. Dahdolan, "Modeling of a novel concentrated solar still enhanced with a porous evaporator and an internal condenser," Sol. Energy **114**, 8–16 (2015).
[22]S. Skullong, S. Kwankaomeng, C. Thianpong, and P. Promvonge, "Thermal performance of turbulent flow in a solar air heater channel with rib-groove tabulators," Int. Commun. Heat Mass Transfer **50**, 34–43 (2014).
[23]G. N. Tiwari, *Solar Energy: Fundamentals, Design, Modeling and Applications* (Alpha Science International, UK, 2015).
[24]A. Bejan, *Advanced Engineering Thermodynamics* (Wiley Interscience, New York, 1988).
[25]H. H. Ozturk, "Experimental determination of energy and exergy efficiency of the solar parabolic-cooker," Sol. Energy **77**, 67–71 (2004).
[26]S. Bouadila, M. Lazaar, S. Skouri, S. Kooli, and A. Farhat, "Energy and exergy analysis of a new solar air heater with latent storage energy," Int. J. Hydrogen Energy **39**(27), 15266–15274 (2014).
[27]R. Nowzari, L. B. Y. Aldabbagh, and F. Egelioglu, "Single and double pass solar heaters with partially perforated cover and packed mesh," Energy **73**, 694–702 (2014).
[28]A. J. Mahmood, L. B. Y. Aldabbagh, and F. Egelioglu, "Investigation of single and double pass solar air heater with transverse fins and a package wire mesh layer," Energy Convers. Manage. **89**, 599–607 (2015).
[29]A. A. El-Sebaii, S. Aboul-Enein, M. R. I. Ramadan, S. M. Shalaby, and B. M. Moharram, "Thermal performance investigation of double pass-finned plate solar air heater," Appl. Energy **88**, 1727–1739 (2011).
[30]T. Alam, R. P. Saini, and J. S. Saini, "Experimental investigation on heat transfer enhancement due to V-shaped perforated blocks in a rectangular duct of solar air heater," Energy Convers. Manage. **81**, 374–383 (2014).
[31]A. Kianifar, S. Z. Heris, and O. Mahian, "Exergy and economic analysis of a pyramid-shaped solar water purification system: Active and passive cases," Energy **38**, 31–36 (2012).
[32]C. Choudhury, P. M. Chauhan, and H. P. Garg, "Performance and cost analysis of two-pass solar air heaters," Heat Recovery Syst. CHP **15**, 755–773 (1995).